

Improved Differential Detection of Chip-Level Differentially Encoded Direct-Sequence Spread-Spectrum Signals

Giulio Colavolpe, *Associate Member, IEEE* and Riccardo Raheli, *Member, IEEE*

Abstract—In a paper by Cavallini *et al.*, chip-level differential encoding/detection for direct-sequence spread-spectrum signals was proposed to cope with frequency-nonselctive fast fading channels. It was shown that, unlike in the additive white Gaussian noise channel, in time-varying fading channels the system performance may be considerably improved, especially when the spreading factor is increased.

In this paper, noncoherent sequence detection, recently proposed by the authors, is the starting point for the derivation of receivers with improved performance with respect to that of standard differential detection. For M -ary phase-shift keying signals, a theoretical analysis is performed and the results are confirmed by means of computer simulation. The performance advantage of taking into account a larger phase memory, with respect to the minimum accounted for by differential detection, is demonstrated. In particular, the amount of phase memory is optimized as a function of the Doppler spread for a Rayleigh frequency-nonselctive fading channel. The robustness in the presence of phase noise is also investigated by means of computer simulation.

Index Terms—Chip-level differential encoding, direct-sequence spread-spectrum signals, noncoherent sequence detection.

I. INTRODUCTION

IN THIS paper, we consider direct-sequence spread-spectrum (DS/SS) transmissions, widely used in code-division multiple-access (CDMA). This technique is very attractive for future generation wireless local loops, mobile to satellite and cellular mobile radio systems. As an example, the third generation mobile radio system according to the International Mobile Communications 2000 (IMT-2000) standard will be based on DS/SS CDMA. For applications in mobile radio channels, it is important to devise simple receiver structures able to efficiently cope with a time-varying fading. Due to the difficulty to perform coherent demodulation, noncoherent detection and in particular differential detection, coupled with differential encoding of the data symbols, are frequently used. However, differential detection is an effective technique when the channel phase is approximately constant within at least two symbol intervals. Therefore, in a frequency-nonselctive time-varying fading channel the usefulness of differential detection is limited to low values of the Doppler spread.

Manuscript received July 31, 2000; revised May 9, 2001; accepted May 9, 2001. The editor coordinating the review of this paper and approving it for publication is J. Cavers. This work was supported in part by Consiglio Nazionale delle Ricerche (CNR), Italy. This paper was presented in part at the URSI Intern. Symp. Signals, Systems and Electronics (ISSSE'01), Tokyo, Japan, July 2001.

The authors are with the Dipartimento di Ingegneria dell'Informazione, Università di Parma, 43100 Parma, Italy.

Publisher Item Identifier S 1536-1276(02)00194-0.

In [1], differential encoding and detection is implemented at chip level rather than data symbol level. With this simple idea, the receiver robustness to high channel dynamics is increased since phase variations do not affect system performance as long as they can be considered negligible within a pair of chip intervals. As observed in [1], this robustness is achieved at the expense of a power penalty, i.e., a performance degradation in terms of signal-to-noise (SNR) ratio necessary to obtain a given value of bit-error probability on the additive white Gaussian noise (AWGN) channel.

In the technical literature, a growing effort has been recently devoted toward the derivation of improved noncoherent detection or decoding schemes which, unlike differential detection, suffer from a minor power penalty when compared to ideal coherent detection (see [2] and references therein). In particular, *noncoherent sequence detection* (NSD), recently proposed by the authors [2]–[4], approximates the optimal noncoherent maximum likelihood sequence detection strategy in order to realize simple suboptimal detection or decoding schemes based on the Viterbi algorithm. With these schemes, the performance approaches that of ideal coherent detection when a *phase memory* parameter N increases. As a special case, differential detection is obtained when $N = 2$.

In this paper, we derive improved differential detection schemes for a DS/SS transmission employing M -ary phase-shift keying (M -PSK) signals and chip-level differential encoding. This modulation format may be useful in applications because of its simplicity and is well suited for a theoretical performance analysis of affordable complexity [4]. Extensions to continuous phase modulations or nonequal energy signaling, such as quadrature amplitude modulations, may be easily dealt with by the methods described in [2], [3]. We consider an AWGN channel, possibly impaired by phase noise and a time-varying frequency-nonselctive Rayleigh fading channel. As intuitively expected, for the AWGN channel the power loss inherent in differential detection may be significantly reduced using values of N greater than 2. Moreover, an improvement over differential detection may be also obtained for a time-varying fading channel. Specifically, the value of N may be optimized for each value of Doppler spread and heuristic rules to calculate the optimal value of N as a function of the spreading factor and the Doppler spread may be derived. The robustness in the presence of phase noise is also investigated by means of computer simulation and the corresponding optimal value of N is derived for some values of phase noise standard deviation.

The paper is organized as follows. In Section II, we describe the transmitted signal and the channel and interference models. The proposed detection algorithms are derived in Section III. A theoretical performance analysis is described in Section IV, considering the relevant cases of the AWGN and Rayleigh fading channels and using a classical upper bound. In Section V, numerical results are presented. Finally, conclusions are drawn in Section VI.

II. SYSTEM MODEL

The assumed modulator block diagram is shown in Fig. 1. An information sequence $\{a_n\}$, composed of independent and identically distributed symbols belonging to an M -ary PSK alphabet, i.e., $a_n \in \{e^{j2\pi i/M}, i = 0, 1, \dots, M-1\}$, is first oversampled by a spreading factor Q and then multiplied by a pseudo-noise (PN) spreading code sequence $\{d_k\}$, obtaining a sequence of symbols $\{b_k\}$ with rate $1/T_c \triangleq Q/T$, T and T_c being the symbol and chip intervals, respectively. Chip symbols $\{d_k\}$ belong to the alphabet $\{\pm 1\}$ and the spreading code sequence is periodic with period L . Symbols $\{b_k\}$ may be expressed as $b_k = a_{\lfloor k/Q \rfloor} d_{\lfloor k/L \rfloor}$, where $\lfloor x \rfloor$ is the integer part of x and $\lfloor x \rfloor_L$ denotes a modulo L operation. These symbols are differentially encoded into a sequence of symbols $c_k = c_{k-1} b_k$, which linearly modulates a shaping pulse $p(t)$ with square-root raised-cosine frequency response of bandwidth $(1 + \alpha)/2T_c$, where α is the rolloff factor. The complex envelope $s(t)$ of the transmitted signal may be expressed as

$$s(t) = \sum_{k=0}^{KQ-1} c_k p(t - kT_c) = \sum_{n=0}^{K-1} \sum_{i=0}^{Q-1} c_{nQ+i} p[t - (nQ+i)T_c]. \quad (1)$$

where K is the number of transmitted symbols. In (1), we have expressed index k in terms of two indices, n and i , which denote the information symbol interval and the chip position, respectively.

The signal $s(t)$ is transmitted over a frequency-nonselctive fading channel, represented by a multiplicative complex fading gain $h(t)$. In the case of Rice fading, $h(t)$ is modeled as a complex, Gaussian process with independent real and imaginary components, mean η_h and variance σ_h^2 . The special cases of AWGN and Rayleigh fading channels can be derived from the Rice fading model by letting $\sigma_h^2 = 0$ or $\eta_h = 0$, respectively. The power spectrum of the fading process $h(t)$ is modeled according to isotropic scattering [5], i.e., the fading autocorrelation function is assumed equal to $R_h(\tau) = \sigma_h^2 J_0(2\pi f_D \tau)$, where $J_0(\cdot)$ is the Bessel function of zeroth order. The fading rate depends on the normalized Doppler rate $f_D T$, where f_D is the maximum Doppler shift. The transmitted signal also undergoes a phase rotation θ , modeled as a random variable with uniform distribution in the interval $[0, 2\pi)$, independent of $h(t)$.

The complex envelope of the received signal may be expressed as

$$r(t) = h(t)e^{j\theta} s(t) + I(t) + w(t) \quad (2)$$

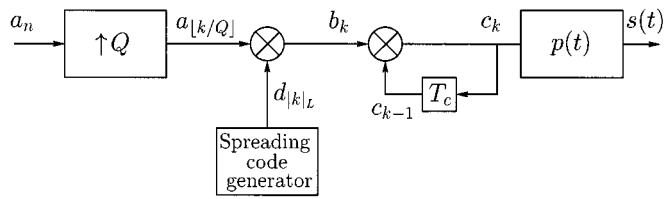


Fig. 1. Modulator block diagram.

where $I(t)$ represents the interference arising from the coexistence of different users on the same bandwidth and $w(t)$ is a complex-valued Gaussian white noise process with independent components, representing the baseband equivalent of bandpass noise with two-sided power spectral density $N_0/2$. Letting $n(t) \triangleq I(t) + w(t)$, if the number of interfering users is large and power control is adopted, the interference may be assumed Gaussian [1], [6]. As in [1], we make the further approximation that $I(t)$ has a flat power spectral density I_0 . Therefore, the total noise process $n(t)$ is assumed complex-valued, Gaussian and white with independent components, each with two-sided power spectral density $N'_0 = N_0 + I_0$.

This model can be generalized to frequency-selective fading channels by considering delayed replicas of the first term in (2) affected by independent multiplicative fading processes.

III. DETECTION ALGORITHMS

In the derivation of the receiver structures, besides a frequency nonselective channel, following [7] we assume a slowly fading model. In this case, it may be easily shown that sampling the output of a filter matched to the shaping pulse $p(t)$ (chip matched filter, CMF) with one sample per chip interval yields a sufficient statistic for optimal detection of the information sequence. Denoting by x_k this sampled output,¹ for both AWGN or Rayleigh fading channels the sequence metric to be maximized is [7]

$$\Gamma_K(\tilde{\mathbf{a}}) = \left| \sum_{k=0}^{KQ-1} x_k \tilde{c}_k^* \right|^2 = \left| \sum_{n=0}^{K-1} \sum_{i=0}^{Q-1} x_{nQ+i} \tilde{c}_{nQ+i}^* \right|^2 \quad (3)$$

where vector $\tilde{\mathbf{c}} = (\tilde{c}_0, \tilde{c}_1, \dots, \tilde{c}_{KQ-1})$ is a hypothetical sequence of transmitted differentially encoded symbols and $\tilde{\mathbf{a}}$ denotes the corresponding hypothetical sequence of information symbols. In other words, the receiver will decide for the sequence $\tilde{\mathbf{a}}$ which maximizes the sequence metric $\Gamma_K(\tilde{\mathbf{a}})$. This sequence metric is equivalent to the following (see (10) and (11) in [2])

$$\begin{aligned} \Lambda_K(\tilde{\mathbf{a}}) &= \sum_{k=0}^{KQ-1} \operatorname{Re} \left\{ x_k \tilde{c}_k^* \sum_{m=0}^{k-1} x_m^* \tilde{c}_m \right\} \\ &= \sum_{n=0}^{K-1} \operatorname{Re} \left\{ \sum_{i=0}^{Q-1} x_{nQ+i} \tilde{c}_{nQ+i}^* \sum_{m=0}^{nQ+i-1} x_m^* \tilde{c}_m \right\} \end{aligned} \quad (4)$$

¹We recall that the choice of $p(t)$ as in Section II assures the absence of interchip interference (ICI).

where we have used the previous expression for index k in terms of indices n and i . This path metric may be recursively computed as a sum of incremental metrics of the form

$$\Delta_n(\tilde{\mathbf{a}}) = \text{Re} \left\{ \sum_{i=0}^{Q-1} \sum_{m=0}^{nQ+i-1} x_{nQ+i} x_m^* \tilde{c}_{nQ+i}^* \tilde{c}_m \right\}. \quad (5)$$

These incremental metrics are characterized by unlimited memory. In fact, expressing (5) in terms of the transmitted symbols, it can be seen that (5) depends not only on the current information symbol a_n but also on all the previous ones [2]. For this reason, the maximization of the sequence metric (4) requires a search on a tree diagram with branch metrics given by (5).

As in [2], [3], and [7], a truncation of this memory allows us to search a trellis diagram by means of a Viterbi algorithm. To this end, in (5) we may consider N most recent received samples x_k and transmitted symbols \tilde{c}_k only. After an initial transient period, the resulting approximate truncated-memory branch metrics are

$$\begin{aligned} \lambda_n(\tilde{\mathbf{a}}) &= \text{Re} \left\{ \sum_{i=0}^{Q-1} \sum_{m=nQ+i-N+1}^{nQ+i-1} x_{nQ+i} x_m^* \tilde{c}_{nQ+i}^* \tilde{c}_m \right\} \\ &= \text{Re} \left\{ \sum_{i=0}^{Q-1} \sum_{j=1}^{N-1} x_{nQ+i} x_{nQ+i-j}^* \tilde{c}_{nQ+i}^* \tilde{c}_{nQ+i-j} \right\} \end{aligned} \quad (6)$$

where an appropriate change of index has been used in the inner sum of the last expression. These branch metrics may be expressed as a function of the information symbols. In fact, noting that

$$c_{nQ+i}^* c_{nQ+i-j} = \prod_{l=0}^{j-1} b_{nQ+i-l}^* = \prod_{l=0}^{j-1} d_{nQ+i-l} a_{[n+(i-l)/Q]}^* \quad (7)$$

we have

$$\lambda_n(\tilde{\mathbf{a}}) = \text{Re} \left\{ \sum_{i=0}^{Q-1} \sum_{j=1}^{N-1} x_{nQ+i} x_{nQ+i-j}^* \cdot \prod_{l=0}^{j-1} d_{nQ+i-l} \tilde{a}_{[n+(i-l)/Q]}^* \right\} \quad (8)$$

According to (8), a trellis state may be defined as

$$\sigma_n = (\tilde{a}_{n-1}, \tilde{a}_{n-2}, \dots, \tilde{a}_{n-\lfloor(N-2)/Q\rfloor}) \quad (9)$$

and the receiver may be based on a Viterbi algorithm with branch metrics (8). Note that despreading is embedded in the branch metrics of the Viterbi algorithm. As in [2], [3], [7], we refer to the integer N as *phase memory*. By extending the theoretical analysis in [4], it can be shown that, on an AWGN channel, when $N \rightarrow \infty$, the performance of the proposed NSD-based receiver tends to that of the optimal coherent detector, under the Gaussian interference assumption.

The number of states $S = M^{\lfloor(N-2)/Q\rfloor}$ depends exponentially on N , but techniques for complexity reduction may be used. In fact, as in [2], [3], the state complexity of the proposed detection schemes may be limited by reduced-state sequence detection (RSSD) [8]–[10]. This technique allows to choose independently the two parameters: phase memory N and number of states S of the Viterbi algorithm. In the limit, the state complexity may be reduced to $S = 1$ and symbol-by-symbol detection *with* decision feedback performed.

A symbol-by-symbol receiver *without* decision feedback may be obtained by a further memory truncation, i.e., by considering, in the expression of the branch metric (8), the previous received samples related to the current information symbol only. In this case, (8) becomes

$$\gamma_n(\tilde{a}_n) = \text{Re} \left\{ \sum_{i=0}^{Q-1} \sum_{j=1}^{\min\{N-1, i+1\}} x_{nQ+i} x_{nQ+i-j}^* \tilde{a}_n^{*j} \cdot \prod_{l=0}^{j-1} d_{nQ+i-l} \right\}. \quad (10)$$

Note that the upper index of the inner sum has been modified with respect to (8) in order to avoid, in the expression of the branch metric, the presence of previous information symbols. Therefore, the detection strategy may be expressed as in (11) at the bottom of the page, where \hat{a}_n denotes the decision on information symbol a_n . For binary PSK (BPSK) and $N = 2$, this receiver reduces to that proposed in [1] as a special case. The different form of memory truncation in (8) and (10) is depicted in Fig. 2, where $\gamma_n(\tilde{a}_n)$ is computed using an increasing window size which avoids the presence of previous information symbols, until the maximum value of N chip intervals is reached. On the contrary, $\lambda_n(\tilde{\mathbf{a}})$ is computed using a sliding window of fixed length N .

It is straightforward to show that the two receivers obtained from (11) by choosing $N = M$ and $N = M + 1$ (or, in general, $N = kM$ and $N = kM + 1$, $k = 1, 2, \dots$) differ for terms independent of \tilde{a}_n . Therefore, in both cases the same performance is obtained. In particular, in the case of a BPSK ($M = 2$), no improvement may be obtained in the bit error rate by using an odd value of N with respect to the previous even value.

$$\begin{aligned} \hat{a}_n &= \arg \max_{\tilde{a}_n} \{ \gamma_n(\tilde{a}_n) \} \\ &= \arg \max_{\tilde{a}_n} \left\{ \text{Re} \left[\sum_{i=0}^{Q-1} \sum_{j=1}^{\min\{N-1, i+1\}} x_{nQ+i} x_{nQ+i-j}^* \tilde{a}_n^{*j} \prod_{l=0}^{j-1} d_{nQ+i-l} \right] \right\} \end{aligned} \quad (11)$$

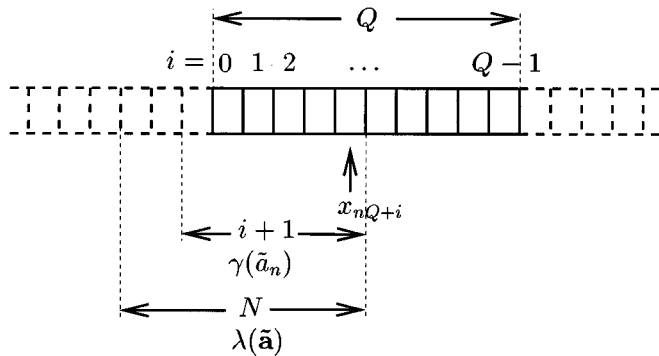


Fig. 2. Memory truncation strategies in metrics (8) and (10).

The receivers with branch metrics (8) or (10) may also be used when symbols a_n account for channel coding. In this case, receivers based on branch metrics (10) operate on the code trellis, whereas receivers based on branch metrics (8) search a trellis diagram defined in terms of the joint code and phase memory, with possible state-complexity reduction, as shown in [2].

In the case of frequency-selective fading channels, the proposed detectors can still be employed because the despreading operation reduces significantly the interference due to the delayed paths, which contribute to the overall interference represented by the second term in (2). Enhanced detectors can also be conceived based on the concept of resolving the multipath components by means of a rake receiver [11] and exploiting the inherent fading diversity in proper branch metrics composed of additive terms.

IV. PERFORMANCE ANALYSIS

Assuming absence of ICI and ideal chip timing, the samples at the output of a CMF may be expressed as

$$x_k = h_k e^{j\theta} c_k + n_k \quad (12)$$

in which $h_k \triangleq h(kT_c)$ and $n_k \triangleq n(t) \otimes p^*(-t)|_{kT_c}$, where \otimes denotes convolution and $p^*(-t)$ is the impulse response of the CMF. The expression of samples x_k given by (12) is correct for slow fading. In the presence of time-varying fading, (12) is a good approximation for small values of Doppler rate $f_D T$. Under the described assumption on the interference, samples n_k are independent, identically distributed, zero-mean, complex, Gaussian random variables with independent real and imaginary components, each with variance $\sigma^2 = N'_0 Q / 2E_b \log_2 M$, where E_b is the received signal energy per information bit. Without loss of generality, for a Rayleigh fading channel we assume $\sigma_h^2 = 1$. As a consequence, the transmitted and received signal energies per information bit coincide.

Using a classical upper bound, we now show how to compute the probability of bit error for the proposed receivers, based on a Viterbi algorithm with branch metrics (8) or a symbol-by-

symbol receiver according to (11), in the important cases of AWGN and Rayleigh fading channels. A generalization to the case of Rician fading channels is straightforward. In the following, we denote by $\mathbf{a} \triangleq \{a_n\}$ and $\hat{\mathbf{a}} \triangleq \{\hat{a}_n\}$, the transmitted and the detected information sequence, respectively. We remark that the noncoherent nature of the considered schemes is due to the presence of terms of the form $x_i x_j^*$ in the detection metrics. As a consequence, a constant phase shift θ does not affect the receiver performance—in the following derivation, $\theta = 0$ is assumed.

A. AWGN Channel and Symbol-by-Symbol Receiver

For an AWGN channel, the expression of samples x_k , assuming $\theta = 0$, is

$$x_k = c_k + n_k. \quad (13)$$

Considering the symbol-by-symbol detection strategy (11) and using the classical union bound, the probability of bit error may be upper bounded by [11]

$$P_b \leq \frac{1}{M \log_2 M} \sum_{a_n} \sum_{\hat{a}_n \neq a_n} b(a_n, \hat{a}_n) P(a_n \rightarrow \hat{a}_n) \quad (14)$$

in which $b(a_n, \hat{a}_n)$ is the number of bit errors when a_n is transmitted and \hat{a}_n is detected and $P(a_n \rightarrow \hat{a}_n)$ is the pairwise error probability defined as

$$P(a_n \rightarrow \hat{a}_n) \triangleq P\{\gamma_n(\hat{a}_n) > \gamma_n(a_n)\}. \quad (15)$$

Assuming Gray labeling, the inner sum in (14) is independent of the transmitted symbol a_n . Therefore, the upper bound on the probability of bit error may be computed assuming symbol $a_n = 1$ is transmitted in the n th signaling interval, i.e.,

$$P_b \leq \frac{1}{\log_2 M} \sum_{\hat{a}_n \neq 1} b(1, \hat{a}_n) P(1 \rightarrow \hat{a}_n). \quad (16)$$

Note that, for binary signaling, the right hand sides of (14) or (16) are the *exact* expressions of the bit error probability.

The pairwise error probability $P(a_n \rightarrow \hat{a}_n)$ may be computed using the methods described in [1], [4]. In fact, the decision variable y defined as [4]

$$y \triangleq \gamma_n(\hat{a}_n) - \gamma_n(a_n) \quad (17)$$

allows us to calculate the pairwise error probability as $P(a_n \rightarrow \hat{a}_n) = P\{y > 0\}$ and may be expressed in the form

$$y = \mathbf{x}^H \mathbf{A} \mathbf{x} \quad (18)$$

where $[\cdot]^H$ is the transpose conjugate operator, $\mathbf{A} = \{A_{ij}\}$, $i, j = -1, 0, 1, \dots, Q-1$, is a Hermitian $(Q+1) \times (Q+1)$ matrix whose elements are²

$$[\mathbf{A}]_{ij} = \begin{cases} \hat{c}_{nQ+i}\hat{c}_{nQ+j}^* - c_{nQ+i}^*c_{nQ+j}^*, & \text{for } 0 < |i-j| \leq N-1 \\ 0, & \text{otherwise} \end{cases} \quad (19)$$

in which $\{c_k\}$ and $\{\hat{c}_k\}$ are the sequences of transmitted symbols corresponding to \mathbf{a} and $\hat{\mathbf{a}}$, respectively and

$$\mathbf{x} \triangleq (x_{nQ-1}, x_{nQ}, x_{nQ+1}, \dots, x_{nQ+Q-1})^T. \quad (20)$$

Conditionally on a specific transmitted sequence, vector \mathbf{x} has independent complex Gaussian components x_k , given by (13), with mean c_k and variance $2\sigma^2$. Its conditional mean vector and covariance matrix are

$$\begin{aligned} \boldsymbol{\eta}_{\mathbf{x}} &\triangleq E\{\mathbf{x}\} \\ &= (c_{nQ-1}, c_{nQ}, c_{nQ+1}, \dots, c_{nQ+Q-1})^T \\ \mathbf{C}_{\mathbf{x}} &\triangleq E\{(\mathbf{x} - \boldsymbol{\eta}_{\mathbf{x}})(\mathbf{x} - \boldsymbol{\eta}_{\mathbf{x}})^H\} \\ &= 2\sigma^2 \mathbf{I} \end{aligned} \quad (21)$$

where \mathbf{I} denotes the identity matrix.

The Hermitian matrix \mathbf{A} may be diagonalized as $\mathbf{A} = \mathbf{P}\mathbf{M}\mathbf{P}^{-1}$, where $\mathbf{M} \triangleq \text{diag}(\mu_i)$ is the diagonal eigenvalue matrix of \mathbf{A} (μ_i denotes the i th eigenvalue), \mathbf{P} is unitary (i.e., $\mathbf{P}^{-1} = \mathbf{P}^H$) and its columns are the eigenvectors of \mathbf{A} . Since \mathbf{A} is Hermitian, its eigenvalues are real. The quadratic form (18) may be expressed as

$$y = \mathbf{x}^H \mathbf{A} \mathbf{x} = \mathbf{x}^H \mathbf{P} \mathbf{M} \mathbf{P}^{-1} \mathbf{x} = \mathbf{z}^H \mathbf{M} \mathbf{z} = \sum_{i=1}^E \mu_i |z_i|^2 \quad (22)$$

in which $\mathbf{z} \triangleq \mathbf{P}^{-1} \mathbf{x} = \mathbf{P}^H \mathbf{x}$ and E denotes the number of nonzero eigenvalues.

The random vector \mathbf{z} is Gaussian with mean vector and covariance matrix given by

$$\begin{aligned} \boldsymbol{\eta}_{\mathbf{z}} &\triangleq E\{\mathbf{z}\} \\ &= \mathbf{P}^{-1} \boldsymbol{\eta}_{\mathbf{x}} \\ &= \mathbf{P}^H (c_{nQ-1}, c_{nQ}, c_{nQ+1}, \dots, c_{nQ+Q-1})^T \\ \mathbf{C}_{\mathbf{z}} &\triangleq E\{(\mathbf{z} - \boldsymbol{\eta}_{\mathbf{z}})(\mathbf{z} - \boldsymbol{\eta}_{\mathbf{z}})^H\} \\ &= \mathbf{P}^H E\{(\mathbf{x} - \boldsymbol{\eta}_{\mathbf{x}})(\mathbf{x} - \boldsymbol{\eta}_{\mathbf{x}})^H\} \mathbf{P} \\ &= 2\sigma^2 \mathbf{I}. \end{aligned} \quad (23)$$

Therefore, z_i are complex, Gaussian, independent random variables with nonzero mean and $|z_i|^2$ have a noncentral chi-square distribution with two degrees of freedom [11], [12]. As shown

²In order to simplify the notation, indices i and j are allowed to take on values which start from -1 because the last sample belonging to the previous interval appears in the expression of the detection strategy (11).

in [4] the bilateral Laplace transform of the probability density function of y may be expressed as

$$\Psi_y(s) = \prod_{i=1}^E \frac{-p_i}{s-p_i} \exp\left\{\frac{ss_i p_i}{s-p_i}\right\} \quad (24)$$

where $s_i \triangleq \mu_i |\eta_{z_i}|^2$ and $p_i \triangleq -1/2\mu_i \sigma^2$.

Since a closed-form expression of the probability density function of y does not exist, for the evaluation of $P(a_n \rightarrow \hat{a}_n)$ one could use $\Psi_y(s)$ and the residue theorem as in [13]. Unfortunately, the singularities of the function $\Psi_y(s)$ are *essential* and their residues may not be expressed in closed-form. Therefore, in order to compute the pairwise error probability, one of the numerical methods known in the literature has to be employed (see [4] and references therein). We used *saddlepoint integration*, based on a numerical integration of $\Psi_y(s)$ on the complex plane [14].

B. Rayleigh Fading Channel and Symbol-by-Symbol Receiver

For a Rayleigh fading channel, the expression of samples x_k , assuming $\theta = 0$, is

$$x_k = h_k c_k + n_k. \quad (25)$$

Considering the detection strategy (11), expressions (14)–(20) also hold in this case, the difference being in the statistics of \mathbf{x} only. In fact, for a Rayleigh fading channel, conditionally on a specific transmitted sequence, vector \mathbf{x} has complex Gaussian components x_k , given by (25), with zero mean and covariance matrix $\mathbf{C}_{\mathbf{x}} \triangleq E\{\mathbf{x}\mathbf{x}^H\}$, whose generic element is

$$[\mathbf{C}_{\mathbf{x}}]_{ij} = E\{x_i x_j^*\} = c_i c_j^* \sigma_h^2 J_0[2\pi f_D(i-j)T_c] + 2\sigma^2 \delta_{ij} \quad (26)$$

in which δ_{ij} is the Kronecker delta. Proceeding as in [1], [15], we first diagonalize the nonnegative definite Hermitian matrix $\mathbf{C}_{\mathbf{x}}$ as

$$\mathbf{C}_{\mathbf{x}} = \mathbf{T} \mathbf{D} \mathbf{T}^{-1} = \mathbf{T} \mathbf{D}_1 \mathbf{D}_1 \mathbf{T}^{-1} \quad (27)$$

where $\mathbf{D} = \text{diag}(\delta_i)$ is the diagonal eigenvalue matrix of $\mathbf{C}_{\mathbf{x}}$, $\mathbf{D}_1 = \text{diag}(\sqrt{\delta_i})$,³ and \mathbf{T} is the unitary matrix of its eigenvectors. Defining

$$\mathbf{u} \triangleq \mathbf{D}_1^{-1} \mathbf{T}^{-1} \mathbf{x} \quad (28)$$

the decision variable y becomes

$$y = \mathbf{x}^H \mathbf{A} \mathbf{x} = \mathbf{u}^H \mathbf{D}_1 \mathbf{T}^H \mathbf{A} \mathbf{T} \mathbf{D}_1 \mathbf{u} = \mathbf{u}^H \mathbf{A}' \mathbf{u} \quad (29)$$

where $\mathbf{A}' \triangleq \mathbf{D}_1 \mathbf{T}^H \mathbf{A} \mathbf{T} \mathbf{D}_1$. Vector \mathbf{u} is Gaussian, with zero mean and covariance matrix

$$\mathbf{C}_{\mathbf{u}} = E\{\mathbf{u}\mathbf{u}^H\} = \mathbf{D}_1^{-1} \mathbf{T}^{-1} E\{\mathbf{x}\mathbf{x}^H\} \mathbf{T} \mathbf{D}_1^{-1} = \mathbf{I}. \quad (30)$$

Therefore, the problem is now similar to that solved in the previous section and the same methods to compute the pairwise

³Note that matrix $\mathbf{C}_{\mathbf{x}}$ is Hermitian and nonnegative definite. Therefore, δ_i are real and $\delta_i \geq 0$, for all i . In the following, we assume $\delta_i > 0$, for all i , as this assumption is verified for the considered values of normalized Doppler rate.

error probability may be used with a difference only. In fact, in the case of a Rayleigh fading channel, vector \mathbf{u} has zero mean. As a consequence, after a transformation similar to (22) applied to the quadratic form $\mathbf{u}^H \mathbf{A}' \mathbf{u}$, the decision variable may be expressed as a linear combination of independent random variables with *central* chi-square distribution with two degrees of freedom. Denoting by $\mu'_i, i = 1, 2, \dots, E'$, the nonzero eigenvalues of \mathbf{A}' and defining $p'_i \triangleq 1/2\mu'_i$, the bilateral Laplace transform of the probability density function of the decision variable is now

$$\Psi_y(s) = \prod_{i=1}^{E'} \frac{-p'_i}{s - p'_i}. \quad (31)$$

As a consequence, its singularities are not essential and the residues may be expressed in closed form [13].

C. Receiver Based on a Viterbi Algorithm

For a Viterbi receiver with branch metrics (8) [or (10) if a channel code is present] without state-complexity reduction and for both AWGN and Rayleigh fading channels, the upper bound⁴ on the probability of bit error becomes [16]

$$P_b \leq \frac{1}{\log_2 M} \sum_{\mathbf{a}} P(\mathbf{a}) \sum_{\hat{\mathbf{a}} \neq \mathbf{a}} b(\mathbf{a}, \hat{\mathbf{a}}) P(\mathbf{a} \rightarrow \hat{\mathbf{a}}) \quad (32)$$

in which $b(\mathbf{a}, \hat{\mathbf{a}})$ is the number of bit errors entailed by the error event $(\mathbf{a}, \hat{\mathbf{a}})$, $P(\mathbf{a} \rightarrow \hat{\mathbf{a}})$ is the pairwise error probability and $P(\mathbf{a})$ is the a priori probability of sequence \mathbf{a} . The pairwise error probability $P(\mathbf{a} \rightarrow \hat{\mathbf{a}})$ is the probability that the sum of the branch metrics $\lambda_k(\hat{\mathbf{a}})$ relative to the erroneous path exceeds the sum of the metrics $\lambda_k(\mathbf{a})$ on the correct path. Denoting by D the number of symbols in which the erroneous and correct paths differ, the duration of the error event is of $D+d$ symbol intervals, where d is related to the definition of trellis state [4]. Therefore, an error event beginning at time n ends at time $n+D+d$. Hence, $P(\mathbf{a} \rightarrow \hat{\mathbf{a}})$ may be expressed in terms of the decision variable

$$y \triangleq \sum_{k=n}^{n+D+d-1} [\lambda_k(\hat{\mathbf{a}}) - \lambda_k(\mathbf{a})]. \quad (33)$$

Even in this case, the pairwise error probability may be expressed as the probability that a quadratic form in a suitable defined vector \mathbf{x} is positive, where \mathbf{x} takes into account the samples at the output of the CMF corresponding to the error event [4]. As a consequence, the methods described in the previous sections may be applied to compute the pairwise error probability in this case, for both AWGN and Rayleigh fading channels. For further details, see [4].

V. NUMERICAL RESULTS

The performance of the proposed decoding algorithms is assessed in terms of bit error rate (BER) versus E_b/N'_0 .

For a quaternary PSK (QPSK) modulation and an AWGN channel, the performance of a symbol-by-symbol noncoherent receiver based on strategy (11) is shown in Fig. 3. A spreading

⁴This bound is sometimes called "union bound," although this terminology is strictly appropriate for the error-event probability.

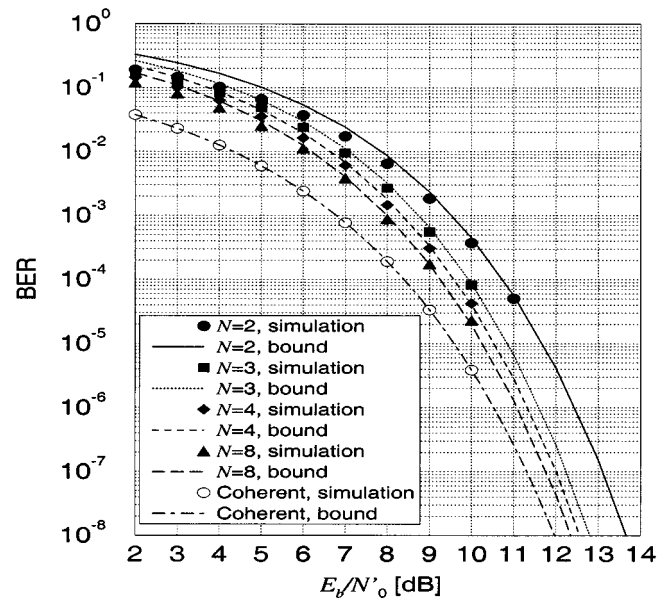


Fig. 3. BER of the proposed symbol-by-symbol noncoherent receiver based on (11) for QPSK and an AWGN channel. $Q = 8$ and various values of N are considered.

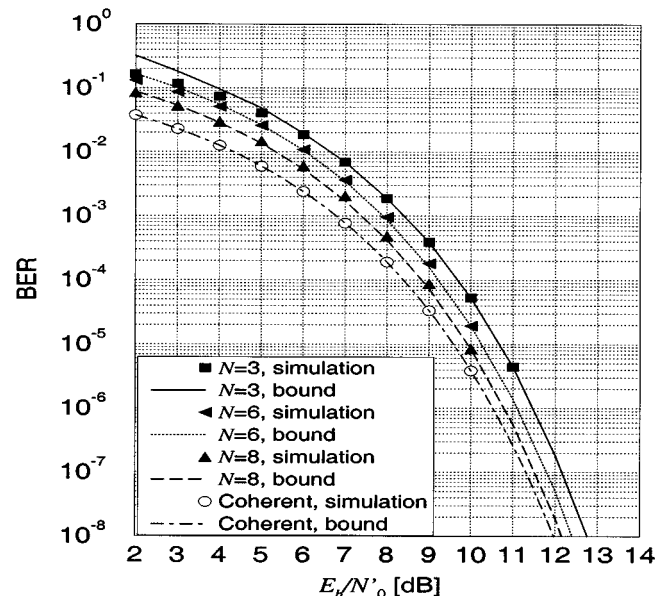


Fig. 4. BER of the proposed noncoherent receiver based on a Viterbi algorithm with branch metrics (8) for QPSK and an AWGN channel. $Q = 8$ and various values of N are considered.

factor $Q = 8$ and various values of N are considered. The performance of a coherent receiver in the absence of chip-level differential encoding is also shown for comparison. In the figure, we may observe a good agreement between simulation and theoretical analysis and a significant improvement in performance by increasing the value of N . In fact, with $N = 8$, the loss with respect to coherent detection is only 0.4 dB at a BER of 10^{-8} . An improvement may be obtained, for a given value of N , by using the noncoherent receiver based on a Viterbi algorithm with branch metrics (8) and $S = 4$ states. The relevant performance is shown in Fig. 4, where bounds are obtained using the

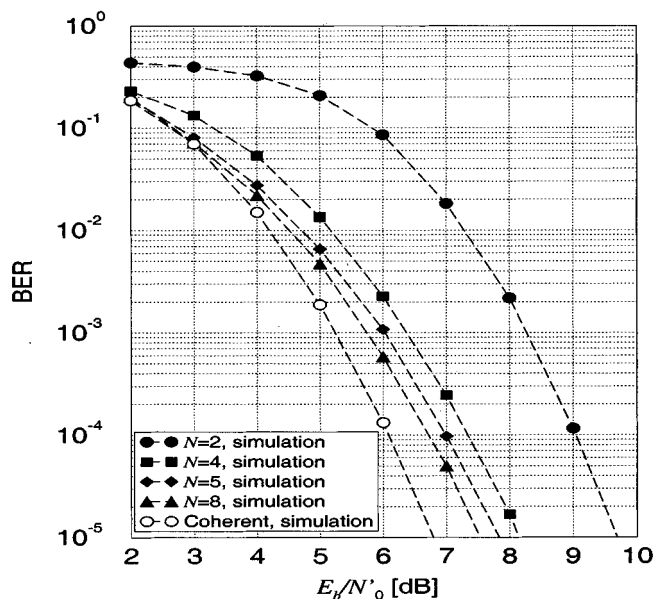


Fig. 5. BER of the proposed detection schemes for 8-state TC-8-PSK and an AWGN channel. $Q = 8$ and various values of N are considered.

upper bound (32) considering small values of D only (i.e., the so-called “truncated upper bound”).

The proposed noncoherent detection strategy has also been applied to trellis-coded modulation (TCM). An 8-state trellis-coded (TC) 8-PSK scheme from [17] is considered for transmission on an AWGN channel and chip-level differential encoding of the spread code symbols is used. The considered receivers operate on the code trellis using the branch metrics (10) with various values of N . A spreading factor $Q = 8$ is assumed. The performance, assessed by computer simulation, is shown in Fig. 5, along with that of a coherent receiver. With $N = 8$ the performance degradation with respect to coherent detection is negligible (0.6 dB at a BER of 10^{-5}).

The performance under dynamic channel conditions has also been investigated assuming $p(t)$ has square-root raised-cosine frequency response with rolloff $\alpha = 0.5$. For a QPSK modulation and a Rayleigh fading channel, the performance of a symbol-by-symbol noncoherent receiver based on strategy (11) is shown in Fig. 6 for $f_D T = 0.1$. A spreading factor $Q = 32$ and various values of N are considered. We may observe that, increasing the phase memory N , a power gain may be achieved with respect to a simple differential detector ($N = 2$). At high values of SNR and BER from 10^{-8} to 10^{-3} , a gain of about 2 dB is obtained for $N = 8$. Further increasing the value of N , the performance degrades and a visible error floor appears for $N = 32$. We may conclude that an optimal value of phase memory N exists for a time varying channel, as a compromise between estimation accuracy, which is achieved for large N and robustness to channel dynamics, which requires a small N . For the considered Doppler rate $f_D T = 0.1$ and spreading factor $Q = 32$, this optimal value is $N = 8$. This optimal value is related with the length of the implicit estimation window [2] and is expected to be approximately proportional to the value of Q .

Even for large values of $f_D T$, a performance improvement may be obtained by increasing the value of N . The performance of the receiver in Fig. 6 is analyzed in Fig. 7 for a fast Rayleigh

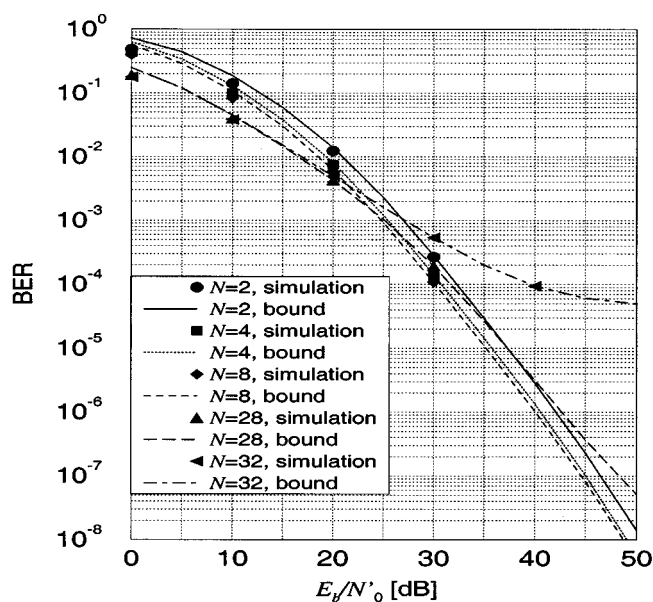


Fig. 6. BER of the proposed symbol-by-symbol noncoherent receiver based on (11) for QPSK and a Rayleigh fading channel with $f_D T = 0.1$. $Q = 32$ and various values of N are considered.

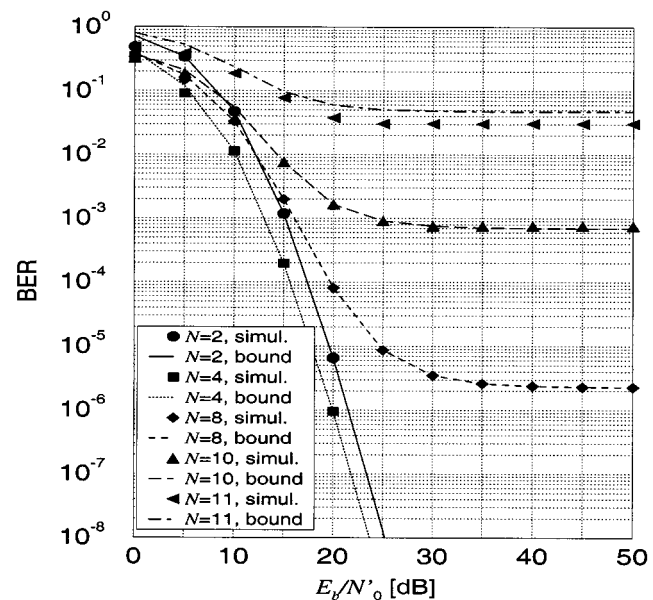


Fig. 7. BER of the proposed symbol-by-symbol noncoherent receiver based on (11) for QPSK and a Rayleigh fading channel with $f_D T = 2$. $Q = 32$ and various values of N are considered.

fading channel with $f_D T = 2$ and a similar behavior is noticed. Specifically, an optimal value of $N = 4$ is observed with a power gain of about 2 dB with respect to differential detection ($N = 2$) at high values of SNR. For increasing values of N beyond the optimal one, an error floor appears. In both Figs. 6 and 7, an excellent agreement between theoretical analysis and computer simulation is observed.

For each value of Doppler rate $f_D T$ and spreading factor Q , the parameter N may be optimized. For BER values of practical interest, the optimal values N_{opt} of N for BPSK and QPSK are given in Tables I and II, respectively. These results may be summarized by means of heuristic expressions. As an example,

TABLE I
OPTIMAL VALUES OF N FOR A BPSK
MODULATION ON A RAYLEIGH FADING CHANNEL

	$Q = 4$	$Q = 8$	$Q = 16$	$Q = 32$	$Q = 64$
$f_D T = 2$	2	2	2	4	6
$f_D T = 1$	2	2	2	4	8
$f_D T = 0.1$	2	2	4	8	16
$f_D T = 0.01$	2	2	6	12	24
$f_D T = 0.001$	2	4	8	16	32

TABLE II
OPTIMAL VALUES OF N FOR A QPSK MODULATION ON A RAYLEIGH
FADING CHANNEL

	$Q = 4$	$Q = 8$	$Q = 16$	$Q = 32$	$Q = 64$
$f_D T = 2$	2	2	2	4	7
$f_D T = 1$	2	2	3	4	8
$f_D T = 0.1$	2	2	4	8	16
$f_D T = 0.01$	2	4	6	12	24
$f_D T = 0.001$	3	4	8	15	30

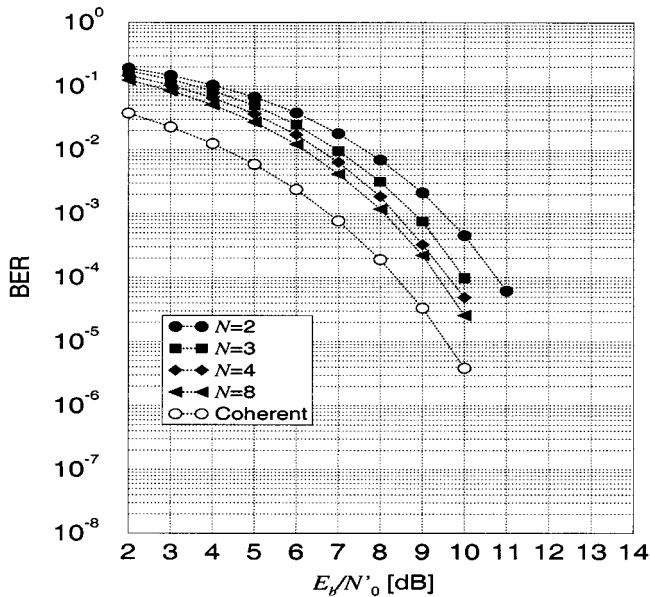


Fig. 8. BER of the proposed receivers based on strategy (11) for QPSK in the presence of phase noise. $Q = 8$ and $\sigma_\Delta = 20^\circ$ are considered.

in the case of BPSK, the optimal values of N may be expressed as

$$N_{\text{opt}} = \max \left\{ 2, 2 \left\lceil \frac{-Q}{16} \log_{10} \frac{f_D T}{10} \right\rceil \right\} \quad (34)$$

which shows a linear dependence of N_{opt} on the spreading factor Q , except for the lower limit $N \geq 2$. This result is in agreement with the intuitive interpretation that the performance actually depends on the length of the time window used for implicit phase estimation [2].

TABLE III
OPTIMAL VALUES OF N FOR A QPSK MODULATION IN THE PRESENCE OF
PHASE NOISE

	$Q = 4$	$Q = 8$	$Q = 16$	$Q = 32$
$\sigma_\Delta = 20$ deg.	4	8	16	32
$\sigma_\Delta = 50$ deg.	2	4	8	14

We also analyzed the performance of the proposed receivers for an AWGN channel in the presence of phase noise, by means of computer simulation. Phase noise is modeled as a time-continuous Wiener phase process with incremental variance over a signaling interval T equal to σ_Δ^2 . The proposed receivers based on strategy (11) are robust to phase noise, as it may be observed in Fig. 8 for QPSK and $Q = 8$. In fact, in Fig. 8 the values of N used in Fig. 3 are considered. Comparing these figures, we may observe that a strong phase noise with standard deviation up to $\sigma_\Delta = 20^\circ$ does not significantly degrade the receiver performance. The optimal values of N for various values of the phase noise standard deviation have also been computed and are shown in Table III.

VI. CONCLUSION

In this paper, noncoherent sequence detection recently proposed by the authors [2], [3] has been used to derive differential detection receivers with improved performance for a DS/SS transmission employing M -PSK signals and chip-level differential encoding. The analysis has been accomplished theoretically and by means of computer simulation. An excellent agreement between theoretical bounds and simulation results has been observed. As expected, an improvement in the receiver performance for an AWGN channel is obtained by using values of phase memory N greater than 2. This is also true for a Rayleigh fading channel with values of normalized Doppler rate of practical significance. In the presence of fading or strong phase noise, or in general for time-varying channels, an optimal value of phase memory exists, at high SNR. This optimal value may be determined using the considered performance bounds for a Rayleigh fading channel and has been determined for various values of the normalized Doppler rate and spreading factor.

REFERENCES

- [1] A. Cavallini, F. Giannetti, M. Luise, and R. Reggiannini, "Chip-level differential encoding/detection of spread-spectrum signals for CDMA radio transmissions over fading channels," *IEEE Trans. Commun.*, vol. 45, pp. 456–463, Apr. 1997.
- [2] G. Colavolpe and R. Raheli, "Noncoherent sequence detection," *IEEE Trans. Commun.*, vol. 47, pp. 1376–1385, Sept. 1999.
- [3] —, "Noncoherent sequence detection of continuous phase modulations," *IEEE Trans. Commun.*, vol. 47, pp. 1303–1307, Sept. 1999.
- [4] —, "Theoretical analysis and performance limits of noncoherent sequence detection of coded PSK," *IEEE Trans. Inform. Theory*, vol. 46, pp. 1483–1494, July 2000.
- [5] R. Clarke, "A statistical theory of mobile radio reception," *Bell Syst. Tech. J.*, vol. 47, pp. 957–1000, 1968.
- [6] M. B. Pursley, "Performance evaluation for phase-coded spread spectrum multiple-access communication—Part I: System analysis," *IEEE Trans. Commun.*, vol. 25, pp. 795–799, Aug. 1977.

- [7] G. Colavolpe and R. Raheli, "Noncoherent sequence detection in frequency nonselective slowly fading channels," *IEEE J. Select Areas Commun.*, vol. 18, pp. 2302–2311, Nov. 2000.
- [8] M. V. Eyuboglu and S. U. H. Qureshi, "Reduced-state sequence estimation with set partitioning and decision feedback," *IEEE Trans. Commun.*, vol. 36, pp. 13–20, Jan. 1988.
- [9] A. Duel-Hallen and C. Heegard, "Delayed decision-feedback sequence estimation," *IEEE Trans. Commun.*, vol. 37, pp. 428–436, May 1989.
- [10] P. R. Chevillat and E. Eleftheriou, "Decoding of trellis-encoded signals in the presence of intersymbol interference and noise," *IEEE Trans. Commun.*, vol. 37, pp. 669–676, July 1989.
- [11] J. Proakis, *Digital Communications*, 2nd ed. New York: McGraw-Hill, 1989.
- [12] M. Schwartz, W. R. Bennet, and S. Stein, *Communication Systems and Techniques*. New York: McGraw-Hill, 1966.
- [13] J. K. Cavers and P. Ho, "Analysis of the error performance of trellis-coded modulations in Rayleigh-fading channels," *IEEE Trans. Commun.*, vol. 40, pp. 74–83, Jan. 1992.
- [14] C. W. Helstrom, *Elements of Signal Detection & Estimation*. Englewood Cliffs, NJ: Prentice Hall, 1995.
- [15] M. E. Rollins and S. J. Simmons, "Simplified per-survivor Kalman processing in fast frequency-selective fading channels," *IEEE Trans. Commun.*, vol. 45, pp. 544–553, May 1997.
- [16] A. J. Viterbi and J. K. Omura, *Principles of Digital Communication and Coding*. New York: McGraw-Hill, 1979.
- [17] G. Ungerboeck, "Channel coding with multilevel/phase signals," *IEEE Trans. Inform. Theory*, vol. IT-28, pp. 55–67, Jan. 1982.

Riccardo Raheli (M'87) received the Dr. Ing. degree (Laurea) in electrical engineering (*summa cum laude*) from the University of Pisa, Italy, in 1983, the M.S. degree in electrical and computer engineering from the University of Massachusetts at Amherst, in 1986, and the Doctoral degree (Perfezionamento) in electrical engineering (*summa cum laude*) from the Scuola Superiore di Studi Universitari e di Perfezionamento (now "S. Anna"), Pisa, Italy, in 1987.

From 1986 to 1988 he was a Project Engineer at Siemens Telecomunicazioni, Cassina de' Pecchi (Milan), Italy. From 1988 to 1991, he was a Research Professor at the Scuola Superiore di Studi Universitari e di Perfezionamento S. Anna, Pisa, Italy. In 1990, he was a Visiting Assistant Professor at the University of Southern California, Los Angeles. Since 1991, he has been at the University of Parma, Italy, where he is currently Professor of Telecommunications. His scientific interests are in the general area of statistical communication theory, with special attention toward digital transmission systems, data-sequence detection techniques, digital signal processing and adaptive algorithms for telecommunications. His research activity has led to numerous scientific publications in leading international journals and conference proceedings and a few industrial patents.

Since 1999, Dr. Raheli has served on the Editorial Board of IEEE TRANSACTIONS ON COMMUNICATIONS as an Editor for Detection, Equalization and Coding.

Giulio Colavolpe (S'97–A'00) was born in Cosenza, Italy, in 1969. He received the Dr. Ing. degree in telecommunications engineering (*cum laude*) from the University of Pisa, Italy, in 1994 and the Doctoral degree in information technology from the University of Parma, Italy, in 1998.

From December 1997 to October 1999, he was a Research Associate at the University of Parma. Since November 1999, he has been a Research Professor at the University of Parma. In 2000, he was Visiting Scientist at the Institut Eurécom, Valbonne, France. His main research interests include digital transmission theory, channel coding, and signal processing.